Available online at www.sciencedirect.com
SCIENCE DIRECT®
ELSEVIER
Icarus 166 (2003) 320–327
ICARUS
www.elsevier.com/locate/icarus

Origin of chaos in the Prometheus–Pandora system

Peter Goldreich [a,b] and Nicole Rappaport [c,*]

[a] *Institute for Advanced Study, Princeton, NJ 08540, USA*
[b] *California Institute of Technology, Pasadena, CA 91125, USA*
[c] *Jet Propulsion Laboratory, California Institute of Technology, Pasadena, CA 91109, USA*

Received 18 June 2003; revised 20 August 2003

Abstract

We demonstrate that the chaotic orbits of Prometheus and Pandora are due to interactions associated with the 121 : 118 mean motion resonance. Differential precession splits this resonance into a quartet of components equally spaced in frequency. Libration widths of the individual components exceed the splitting, resulting in resonance overlap which causes the chaos. Mean motions of Prometheus and Pandora wander chaotically in zones of width 1.8 and 3.1 deg yr^{-1}, respectively. A model with 1.5 degrees of freedom captures the essential features of the chaotic dynamics. We use it to show that the Lyapunov exponent of 0.3 yr^{-1} arises because the critical argument of the dominant member of the resonant quartet makes approximately two separatrix crossings every 6.2 year precessional cycle.

Keywords: Satellites of Saturn; Orbits; Chaos

1. Introduction

Goldreich and Rappaport (2003) (hereafter abbreviated as GR03) showed that the motions of Prometheus and Pandora are chaotic. The chaos arises from their mutual gravitational interactions, which explains why their longitude discrepancies have comparable magnitudes and opposite signs (French et al., 2003). Numerical integrations that account for the full mutual interactions and Saturn's gravitational oblateness yield a Lyapunov exponent of order 0.3 yr^{-1}. GR03 assumed satellite masses scaled to Saturn's mass of 5.80×10^{-10} and 3.43×10^{-10} for Prometheus and Pandora, respectively. These are based on ellipsoidal shapes fit to the satellites by Thomas (1989) and the density of 0.63 $\mathrm{g\,cm}^{-3}$ determined for Saturn's co-orbital satellite Epimetheus by Nicholson et al. (1992).[1] A factor of two is a plausible estimate for the uncertainties in the masses Prometheus and Pandora. We have verified that the Lyapunov exponent is insensitive to the assumed masses within this range, but not far below its lower limit.

GR03's integrations also reproduce qualitative features of the discrepancies between the longitudes of the satellites derived from analysis of recent HST data and predictions based on orbits fit to Voyager images (French et al., 2003). Sudden changes in the mean motions of Prometheus and Pandora are a striking feature of the numerical integrations. These occur at intervals of 6.2 yr when the satellites' apses are anti-aligned. It is notable that the only clearly documented changes in the mean motions occurred around the time of the most recent apse anti-alignment (cf. GR03).

Both in our previous paper (GR03) and in the current one, we neglect interactions of Prometheus and Pandora with other satellites of Saturn. The most significant of these are due to Titan and Mimas. Titan contributes secular perturbations to the orbits of both Prometheus and Pandora. However, these have negligible magnitudes compared to secular perturbations that result from Saturn's oblateness; they are substantially smaller than the uncertainties in these perturbations. Mimas is involved in a near 3 : 2 mean motion resonance with Pandora. In the past we speculated about its possible relevance to estimates of the age of Saturn's rings (Borderies et al., 1984). We intend to revisit this issue in a future publication. However, based on the strength of the resonant terms and the separation from exact resonance, we doubt that interactions with Mimas would affect any of the results of the current investigation.

* Corresponding author.
E-mail address: nicole.j.rappaport@jpl.nasa.gov (N. Rappaport).

[1] We adopt Epimetheus's density because the densities of Prometheus and Pandora are unconstrained by observations.

0019-1035/$ – see front matter
doi:10.1016/j.icarus.2003.09.002

The plan of this paper is as follows. In Section 2 the 121 : 118 mean motion resonance is identified as the probable cause of the chaos. Differential apsidal precession splits this resonance into a quartet of closely spaced components.[2] We describe two new models in which interactions between the satellites are limited to those due to this quartet. The simpler of these reduces the resonant dynamics to a system with one and a half degrees of freedom. Results from these models are compared in Section 3 with those obtained from integrations that account for the full gravitational interactions. Section 4 is devoted to a discussion of the width of the chaotic zone.

2. Origin of chaos

2.1. Resonant quartet

A systematic search for $j : j-k$ mean motion resonances with $k \leqslant 5$ turned up $j = 121$, $k = 3$. This is obvious from the data plotted in Fig. 1.

Following Murray and Dermott (2001), we write the disturbing function for the action of Pandora on Prometheus as

$$\mathcal{R} = \frac{Gm'}{a'}(R_D + \alpha R_E), \tag{1}$$

and that for the action of Prometheus on Pandora as

$$\mathcal{R}' = \frac{Gm}{a'}\left(R_D + \alpha^{-2} R_I\right). \tag{2}$$

Here m and a denote mass and semi-major axis,[3] $\alpha \equiv a/a'$, and G is the gravitational constant. Also, the direct and indirect, exterior and interior, contributions to the dimensionless disturbing function are given by R_D, R_E, and R_I;

$$R_D = \frac{a'}{|\mathbf{r}' - \mathbf{r}|}, \qquad R_E = -\left(\frac{a'}{r'}\right)^3 \frac{\mathbf{r}\cdot\mathbf{r}'}{aa'},$$
$$R_I = -\left(\frac{a}{r}\right)^3 \frac{\mathbf{r}\cdot\mathbf{r}'}{aa'}. \tag{3}$$

To lowest order in the eccentricities, the terms in the literal expansion of the disturbing function associated with a $k = 3$ resonance take the form[4]

$$\begin{aligned} R_D = {} & e^3 f_{82}\cos[121\lambda' - 118\lambda - 3\varpi] \\ & + e^2 e' f_{83}\cos[121\lambda' - 118\lambda - 2\varpi - \varpi'] \\ & + e e'^2 f_{84}\cos[121\lambda' - 118\lambda - \varpi - 2\varpi'] \\ & + e'^3 f_{85}\cos[121\lambda' - 118\lambda - 3\varpi'], \end{aligned} \tag{4}$$

where e, λ, and ϖ stand for eccentricity, mean longitude, and longitude of periapsis. We utilize the expressions for f_{82} to f_{85} that are tabulated in Appendix B of Murray and Dermott (2001). These are written in terms of Laplace coefficients evaluated at α. In the following, j should be viewed as a shorthand for 121:

$$\begin{aligned} f_{82} = \frac{1}{48}\Bigg\{ & \left(-26j + 30j^2 - 8j^3\right) b_{1/2}^{(j)}(\alpha) \\ & + \left(-9 + 27j - 12j^2\right)\alpha \frac{d b_{1/2}^{(j)}(\alpha)}{d\alpha} \\ & + (6 - 6j)\alpha^2 \frac{d^2 b_{1/2}^{(j)}(\alpha)}{d\alpha^2} - \alpha^3 \frac{d^3 b_{1/2}^{(j)}(\alpha)}{d\alpha^3} \Bigg\}, \end{aligned} \tag{5}$$

$$\begin{aligned} f_{83} = \frac{1}{16}\Bigg\{ & \left(-9 + 31j - 30j^2 + 8j^3\right) b_{1/2}^{(j-1)}(\alpha) \\ & + \left(9 - 25j + 12j^2\right)\alpha \frac{d b_{1/2}^{(j-1)}(\alpha)}{d\alpha} \\ & + (-5 + 6j)\alpha^2 \frac{d^2 b_{1/2}^{(j-1)}(\alpha)}{d\alpha^2} \\ & + \alpha^3 \frac{d^3 b_{1/2}^{(j-1)}(\alpha)}{d\alpha^3} \Bigg\}, \end{aligned} \tag{6}$$

$$\begin{aligned} f_{84} = \frac{1}{16}\Bigg\{ & \left(8 - 32j + 30j^2 - 8j^3\right) b_{1/2}^{(j-2)}(\alpha) \\ & + \left(-8 + 23j - 12j^2\right)\alpha \frac{d b_{1/2}^{(j-2)}(\alpha)}{d\alpha} \\ & + (4 - 6j)\alpha^2 \frac{d^2 b_{1/2}^{(j-2)}(\alpha)}{d\alpha^2} \\ & - \alpha^3 \frac{d^3 b_{1/2}^{(j-2)}(\alpha)}{d\alpha^3} \Bigg\}, \end{aligned} \tag{7}$$

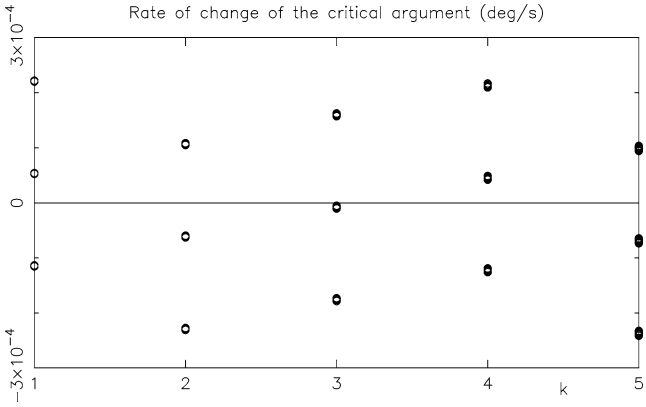

Fig. 1. Rates of change of critical arguments for approximate Prometheus–Pandora mean motion resonances. The plotted points correspond to the best resonances with $j \leqslant 250$ and $k \leqslant 5$. Each resonance of order k is split into a multiplet with $k+1$ members that are equally spaced in frequency. The quartet of $j = 121$, $k = 3$ resonances stands out as the one whose critical argument changes most slowly.

[2] Splitting of mean motion resonances into multiplets is a general feature of the elliptic three-body problem.

[3] Unprimed and primed symbols refer to Prometheus and Pandora, respectively.

[4] To lowest order, only the direct term contributes to $j = 121$ resonances.

Table 1
Masses, initial mean longitudes, and mean motions

Satellite	m/M	Mean longitude (°)	Mean motion (° s^{-1})
Prometheus	5.80×10^{-10}	188.53815	6.797331×10^{-3}
Pandora	3.43×10^{-10}	82.14727	6.629506×10^{-3}

Table 2
Eccentricities, initial apsidal angles, and precession rates

Satellite	Eccentricity	Apsidal angle (°)	Precession rate (° s^{-1})
Prometheus	2.29×10^{-3}	212.85385	3.1911×10^{-5}
Pandora	4.37×10^{-3}	68.22910	3.0082×10^{-5}

Table 3
Resonance arguments, rates of change, periods, and coefficients

Argument	Rate (° s^{-1})	Period (yr)	Coefficient
$121\lambda' - 118\lambda - 3\varpi$	-1.058×10^{-5}	1.078	$e^3 f_{82} = -1.08 \times 10^{-3}$
$121\lambda' - 118\lambda - 2\varpi - \varpi'$	-0.875×10^{-5}	1.303	$e^2 e' f_{83} = 6.26 \times 10^{-3}$
$121\lambda' - 118\lambda - \varpi - 2\varpi'$	-0.692×10^{-5}	1.648	$ee'^2 f_{84} = -1.21 \times 10^{-2}$
$121\lambda' - 118\lambda - 3\varpi'$	-0.509×10^{-5}	2.239	$e'^3 f_{85} = 7.82 \times 10^{-3}$

$$f_{85} = \frac{1}{48}\Bigg\{\big(-6 + 29j - 30j^2 + 8j^3\big) b_{1/2}^{(j-3)}(\alpha) + \big(6 - 21j + 12j^2\big)\alpha \frac{d b_{1/2}^{(j-3)}(\alpha)}{d\alpha} + (-3 + 6j)\alpha^2 \frac{d^2 b_{1/2}^{(j-3)}(\alpha)}{d\alpha^2} + \alpha^3 \frac{d^3 b_{1/2}^{(j-3)}(\alpha)}{d\alpha^3}\Bigg\}. \tag{8}$$

Tables 1 and 2 list values for the parameters used in this paper. Satellite masses are given as fractions of Saturn's mass based on data described in Section 1. Initial values for mean longitudes, apsidal angles, mean motions, and eccentricities are based on orbits fit to Voyager images by Jacobson (personal communication) at epoch 1981 August 23 04:02:12 UTC. Precession rates were calculated from the gravitational field of the Saturnian System (Campbell and Anderson, 1989).

Rates of change of the arguments, corresponding periods, and coefficients for the four terms in Eq. (4) are given in Table 3.

2.2. Numerical integrations

To demonstrate that the quartet of 121 : 118 resonances is the cause of chaos in the Prometheus–Pandora system, we develop two new programs to integrate the satellites' equations of motion. Interactions between the satellites are restricted to the four resonant interaction terms in the Fourier expansion of the disturbing function R_D. Each program propagates the satellites' orbital elements rather than their cartesian coordinates and velocities as is done by the "old program" FSHEP used in GR03.

We adopt epicyclic elliptic elements instead of the more standard osculating elliptic elements since, unlike the latter, they do not require short period terms to describe elliptic orbits around oblate planets (cf. Borderies-Rappaport and Longaretti, 1994; henceforth, referred to as BRL). BRL derive a modified version of Gauss' equations for the elements a_e, e_e, $\varpi_e = \omega_e + \Omega_e$, and $\lambda_e = \varpi_e + M_e$.[5] From these, it is a straightforward exercise to derive a restricted version of Lagrange's equations that is valid in the planar case. We work with a simplified set appropriate for low eccentricity orbits about a modestly oblate planet. They read:[6]

$$\frac{d\lambda}{dt} = \Omega, \tag{9}$$

$$\frac{da}{dt} = \frac{2}{\Omega a}\frac{\partial \mathcal{R}}{\partial \lambda}, \tag{10}$$

$$\frac{d\varpi}{dt} = \Omega - \kappa, \tag{11}$$

$$\frac{de}{dt} = -\frac{1}{\Omega a^2 e}\frac{\partial \mathcal{R}}{\partial \varpi}, \tag{12}$$

where

$$\Omega^2 = \frac{GM}{a^3}\left[1 + \frac{3}{2}\left(\frac{R_p}{a}\right)^2 J_2 - \frac{15}{8}\left(\frac{R_p}{a}\right)^4 J_4 + \frac{35}{16}\left(\frac{R_p}{a}\right)^6 J_6 - \cdots\right], \tag{13}$$

$$\kappa^2 = \frac{GM}{a^3}\left[1 - \frac{3}{2}\left(\frac{R_p}{a}\right)^2 J_2 + \frac{45}{8}\left(\frac{R_p}{a}\right)^4 J_4 - \frac{175}{16}\left(\frac{R_p}{a}\right)^6 J_6 + \cdots\right]. \tag{14}$$

From Campbell and Anderson (1989), $J_2 = 1.6298 \times 10^{-2} \pm 1 \times 10^{-5}$, $J_4 = -9.15 \times 10^{-4} \pm 4 \times 10^{-5}$, and $J_6 = 1.03 \times 10^{-4} \pm 5 \times 10^{-5}$.

2.3. New models

In the planar approximation, the Prometheus–Pandora system has four degrees of freedom and preserves two integrals, the total energy and total angular momentum. Thus

[5] Hereafter we drop the subscript e.

[6] To the order that we are working, it is consistent to apply the expressions for $\mathcal{R}$ given in Section 2.1 with the osculating elements used there taken here to be epicyclic elements.

each phase space trajectory lies on a six dimensional hypersurface embedded in the eight dimensional phase space.

FSHEPRES integrates the four, first-order equations (9)–(12) for each satellite. Thus it differs from FSHEP mainly because it limits the interactions between the satellites to resonant terms.[7] Other minor differences arise because FSHEPRES integrates a simplified set of Lagrange's equations. In particular, the conservation laws are only approximately satisfied.

FSHEPSIM integrates only the first two Eqs. (9) and (10) for each satellite. This drastic simplification is reasonable because, as a consequence of the rapid differential precession caused by Saturn's oblateness, interactions between the satellites produce negligible effects on their apsidal angles and orbital eccentricities (GR03). A further simplification arises because perturbations of a and a' due to terms of the resonant quartet are related by

$$\frac{m}{a^2}\frac{da}{dt} \approx -\frac{m'}{a'^2}\frac{da'}{dt}. \tag{15}$$

It proves convenient to define the variable

$$\psi = 121\lambda' - 118\lambda, \tag{16}$$

so that R_D is expressed as

$$R_D = \sum_{q=1}^{4} C_q \cos(\psi - \delta_q), \tag{17}$$

with $\delta_1 = 3\varpi$, $\delta_2 = 2\varpi + \varpi'$, $\delta_3 = \varpi + 2\varpi'$, $\delta_4 = 3\varpi'$, and each $\dot{\delta}_q$ =constant. The evolution of ψ is governed by

$$\begin{aligned}\frac{d^2\psi}{dt^2} &= 3\left[(121\Omega')^2\frac{m}{M} + \alpha(118\Omega)^2\frac{m'}{M}\right] \\ &\quad\times \sum_{q=1}^{4} C_q \sin(\psi - \delta_q) \qquad (18)\\ &= 3(121\Omega')^2\frac{m}{M}\left[1+\alpha(m'/m)\right] \\ &\quad\times \sum_{q=1}^{4} C_q \sin(\psi - \delta_q), \qquad (19)\end{aligned}$$

where in writing the second form of Eq. (19), we have applied the mean motion resonance relation $\Omega'/\Omega \approx 118/121$ and emphasized the contribution from the lighter body, m'. Individual mean longitudes follow from the relations

$$\begin{aligned}\lambda(t) = &\big(-\alpha(m'/m)\psi(t) + 118\big[\lambda(0) + \dot{\lambda}(0)t\big] \\ &+ 121\alpha(m'/m)\big[\lambda'(0) + \dot{\lambda}'(0)t\big]\big) \\ &\times \big(121\big[1+\alpha(m'/m)\big]\big)^{-1}, \end{aligned}\tag{20}$$

$$\begin{aligned}\lambda'(t) = &\big(\psi(t) + 121\alpha(m'/m)\big[\lambda'(0) + \dot{\lambda}'(0)t\big] \\ &+ 118\big[\lambda(0) + \dot{\lambda}(0)t\big]\big)\big(121\big[1+\alpha(m'/m)\big]\big)^{-1}. \end{aligned}\tag{21}$$

The system of two satellites orbiting an axisymmetric planet has six degrees of freedom and two scalar integrals, energy and angular momentum. Thus each trajectory is confined to a hypersurface in phase space with ten dimensions. By restricting the satellite orbits to the equator plane of an axisymmetric planet, we effected a reduction to four degrees of freedom while maintaining both integrals. In this case each trajectory is restricted to a six dimensional hypersurface in phase space. The approximations just described reduce the number of degrees of freedom to one and the full phase space to two dimensions. However, the extended phase space, which includes a time axis, has three dimensions because no integrals remain.[8] In modern notation, such a system is said to have 1.5 degrees of freedom.

3. Comparison of results

In this section we compare results obtained using FSHEPRES and FSHEPSIM with those obtained with FSHEP. As in GR03, all our simulations are initialized with orbital elements for Prometheus and Pandora taken from Jacobson's ephemerides. Comparisons among similar calculations done with each of the three programs are presented in Figs. 2–7. As a consequence of chaos, qualitative similarities are the best that can be expected. These are apparent in each set of figures. Moreover, we have run each of the three programs several times making slight changes in initial conditions to verify that the results presented in this paper are typical of the output from each program.

The similarity between the 20 year runs of longitude variations displayed in Figs. 2 and 3, while consistent with a Lyapunov exponent slightly smaller than 0.3 yr^{-1} as shown in Fig. 4, probably also reflects the fact that at the Voyager epoch the mean motions of Prometheus and Pandora were close to their respective maximum and minimum. This accounts for the negative values of the rates of each resonant argument quoted in Table 3.

Figure 5 shows that over 3000 years the net variation of $\Phi_3 \equiv 121\lambda' - 118\lambda - \varpi - 2\varpi'$ is much smaller than that of the other critical arguments. Together with the constraint imposed by the conservation of energy on the relative variations of n and n', this implies that the time-averaged value of n over this interval of 3000 years is smaller than its initial value by about 0.67 deg yr^{-1} and that of n' is larger by about 1.14 deg yr^{-1}. The relatively small variation of Φ_3 has a plausible dynamical explanation in terms of the relative amplitudes of the individual terms in the resonant quartet (cf. Table 3). The term with critical argument Φ_3 has the largest amplitude. Amplitudes of the terms with critical arguments Φ_2 and Φ_4 are about half as large and their signs are opposite to that of the Φ_3 term. The amplitude of the term with

[7] We view as an unimportant difference the use of orbital elements by FSHEPRES and cartesian positions and velocities by FSHEP.

[8] The dynamics remains Hamiltonian, but the Hamiltonian is an explicit function of time through the linear dependence of the δ_q on t.

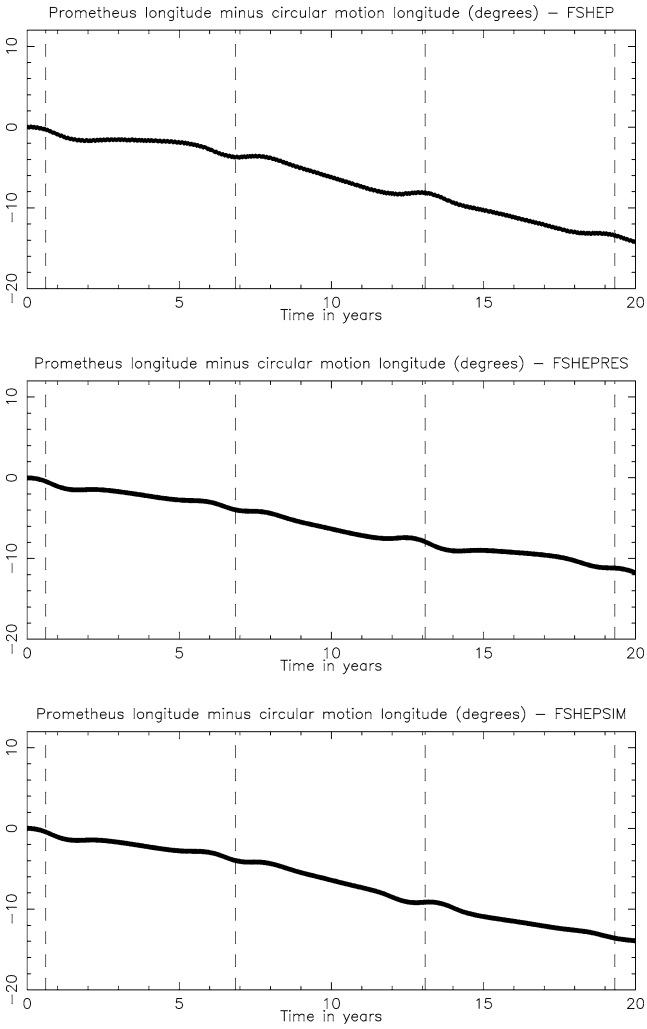

Fig. 2. Prometheus longitude in degrees from numerical integration as a function of time over 20 years. A drift based on the initial mean motion has been subtracted from the longitudes. Dashed lines indicate the times of periapsis antialignment. Results shown in the top, middle, and bottom panels were obtained with the programs FSHEP, FSHEPRES, and FSHEPSIM.

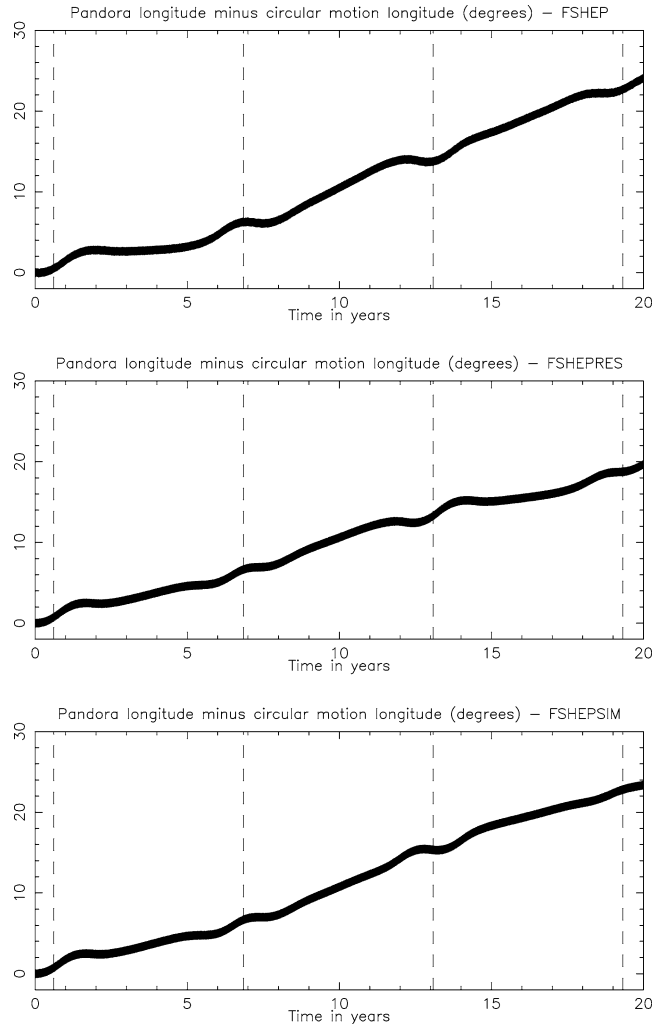

Fig. 3. Pandora longitude in degrees from numerical integration as a function of time over 20 years. A drift based on the initial mean motion has been subtracted from the longitudes. Dashed lines indicate the times of periapsis antialignment. Results shown in the top, middle, and bottom panels were obtained with the programs FSHEP, FSHEPRES, and FSHEPSIM.

critical argument Φ_1 is by far the smallest. A test of our explanation comes from interchanging the values of e and e'. This results in the phase $\Phi_2 \equiv \lambda' - 118\lambda - 2\varpi - \varpi'$ assuming the special status of being the one with the smallest net variation.

Figures 6 and 7 display longitude variations over 3000 years relative to the longitude based on the average mean motion over this interval. These are seen to be bounded by ± 180 degrees. To a good approximation the longitudes undergo one dimensional random walks so the maximum excursions should scale as the square root of time.

4. Discussion

A closer examination of the one-degree of freedom model developed for FSHEP provides additional insight regarding chaos in the Prometheus–Pandora system.

Overlapping resonances are known to produce chaos. Frequencies of individual members of the resonant quartet are spaced by $\dot{\varpi} - \dot{\varpi}' \approx 1.0\ \mathrm{rad\,yr^{-1}}$. This is smaller than the half widths of the individual resonance components.[9] Half widths computed from Eq. (19) and the data in Tables 1–3 are, in order of increasing resonance frequency, $1.5, 3.7, 5.1, 4.1\ \mathrm{rad\,yr^{-1}}$.

Figure 8 shows surfaces of section based on data from 3000 year integrations using FSHEPSIM. A single point with coordinates $\Phi_3 = \psi - \varpi - 2\varpi'$, $\dot{\Phi}_3 = \dot{\psi} - \dot{\varpi} - 2\dot{\varpi}'$ is plotted each time the apses align (every 6.2 yr when $\varpi - \varpi' = 0$ modulo 2π).[10] Nominal values for the satellites' masses were used for the upper panel. The scattering of

[9] The half width is the maximum angular velocity achieved during motion on the separatrix.

[10] We chose apse alignment to minimize the effects of the interaction energy.

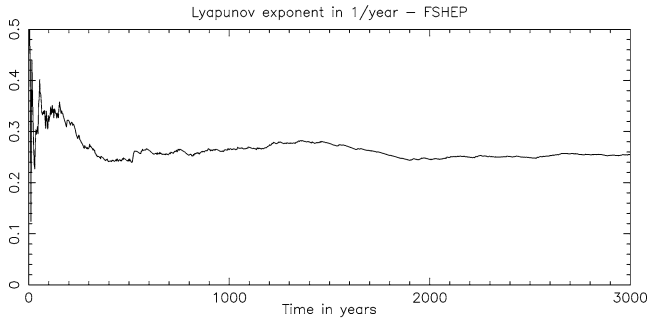

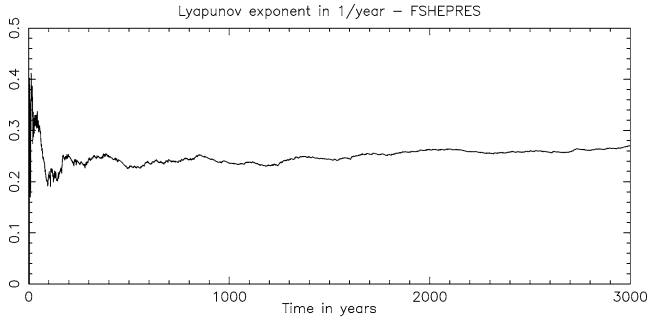

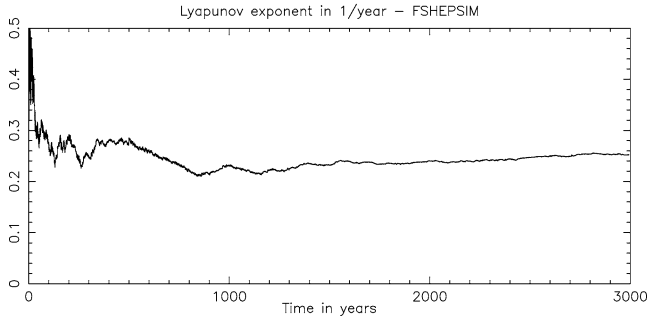

Fig. 4. Lyapunov exponent in yr^{-1} for the Prometheus–Pandora system over a period of 3000 years. The results shown in the top, middle, and bottom panels were obtained with the programs FSHEP, FSHEPRES, and FSHEPSIM.

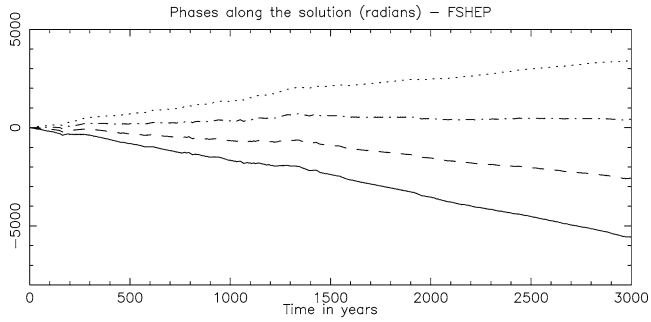

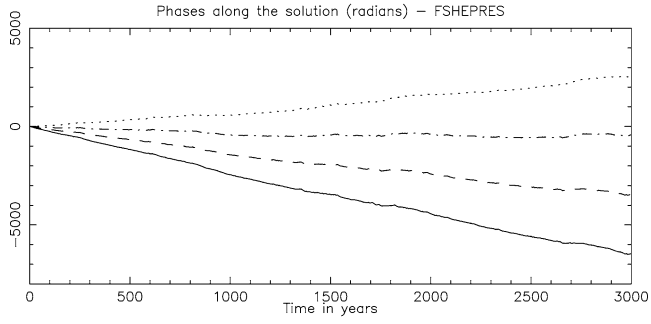

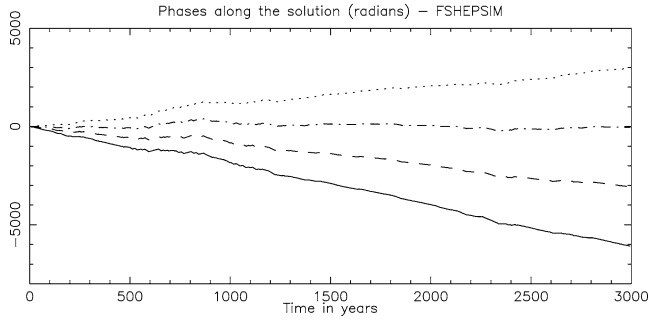

Fig. 5. Critical arguments of the individual components of the resonant quartet in radians along the solution; solid, dashed, dashed–dotted, and dotted lines correspond to components with $q = 1, 2, 3, 4$, respectively. Results shown in the top, middle, and bottom panels were obtained with the programs FSHEP, FSHEPRES, and FSHEPSIM.

points over an area in the phase plane is a signature of chaos. The balance in the number of points above and below the horizontal axis and the overall vertical width of their distribution are a consequence of the dominance of the resonance component with critical argument Φ_3. Satellite masses were reduced by a factor 10 below their nominal values to obtain the regular phase space trajectory whose surface of section is shown in the lower panel.

Variations of n and n' are related to those of $\dot{\psi}$ by

$$\frac{dn}{dt} = \frac{1}{121[1+\alpha(m'/m)]}\frac{d\psi}{dt}, \tag{22}$$

$$\frac{dn'}{dt} = \frac{-\alpha(m'/m)}{118[1+\alpha(m'/m)]}\frac{d\psi}{dt}. \tag{23}$$

Thus the total width in $\dot{\psi}$ corresponds to full width variations $\Delta n \approx 1.8\ \mathrm{deg\,yr}^{-1}$ and $\Delta n' \approx 3.1\ \mathrm{deg\,yr}^{-1}$.

Separatrix crossing is at the heart of chaos. Since the Lyapunov exponent for the Prometheus–Pandora system is of order $0.3\ \mathrm{yr}^{-1}$, we expect to find a separatrix that is crossed at this rate. Two clues help us identify it: Φ_3 undergoes relatively small variations compared to the other critical arguments; mean motion changes occur at intervals of 6.2 yr when the satellites' apses are anti-aligned. The former suggests that the separatrix is to be found in the dynamics of Φ_3, and the latter that it is crossed twice almost every precessional cycle.[11]

It is straightforward to show that

$$\frac{d^2\Phi_3}{dt^2} = -A^2(t)\sin\big[\Phi_3 + \Delta(t)\big], \tag{24}$$

where both $A(t)$ and $\Delta(t)$ vary periodically over the precessional cycle. Moreover, the data in Table 3 imply that

$$A^2(t) \approx 2\sin^2\big[(\varpi - \varpi')/2\big], \tag{25}$$

[11] A precessional cycle has period $2\pi/(\dot{\varpi} - \dot{\varpi}')$.

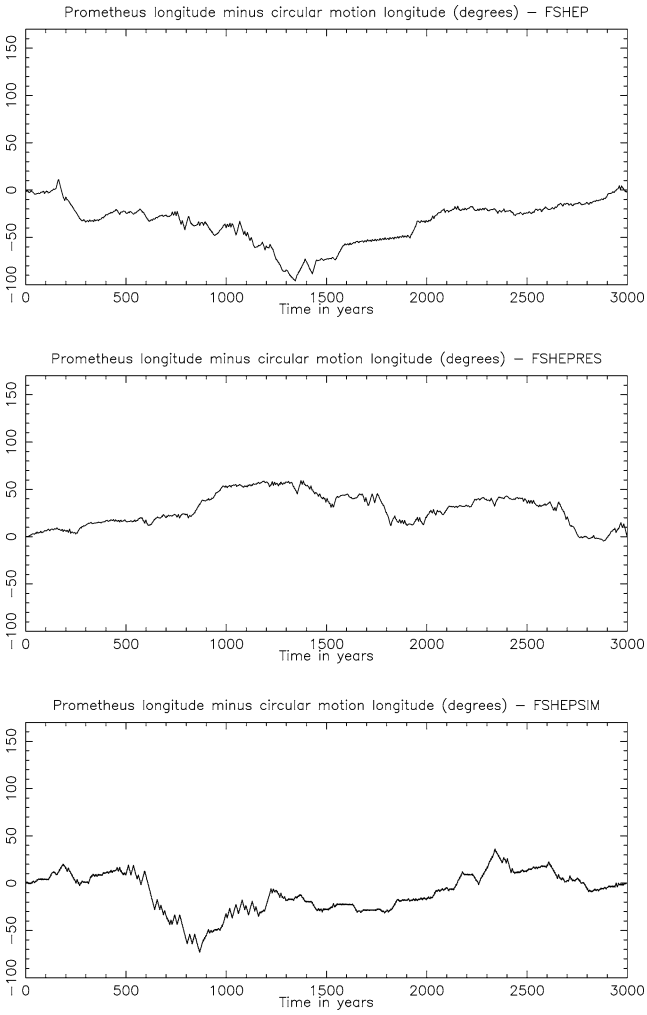

Fig. 6. Prometheus longitude in degrees from numerical integration as a function of time over 3000 years. A drift based on the mean motion averaged over 3000 years has been subtracted from the longitude. Results shown in the top, middle, and bottom panels were obtained with the programs FSHEP, FSHEPRES, and FSHEPSIM.

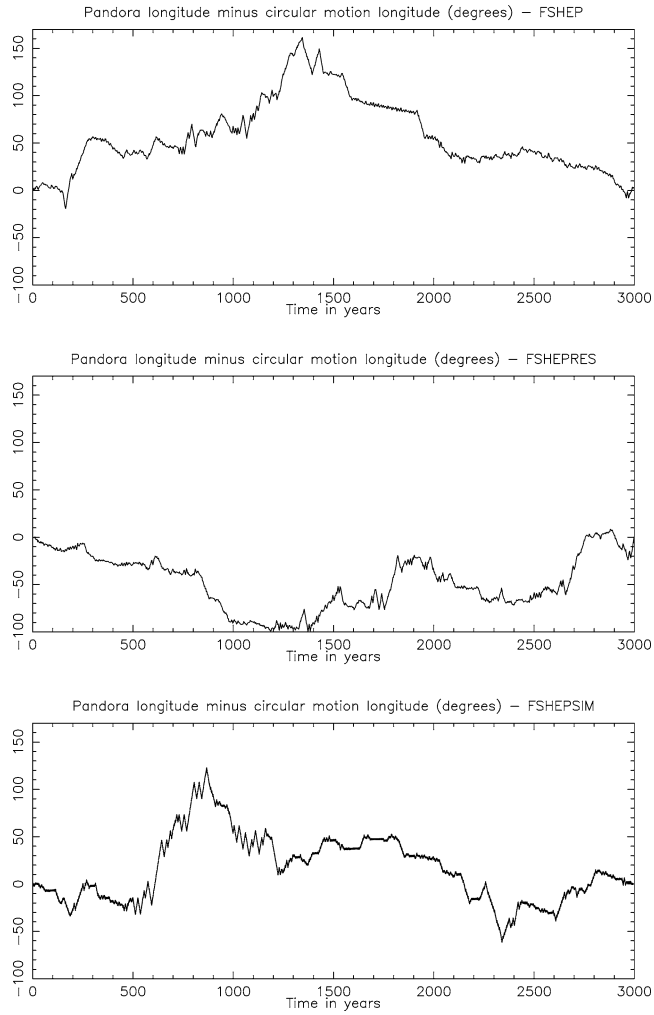

Fig. 7. Pandora longitude in degrees from numerical integration as a function of time over 3000 years. A drift based on the mean motion averaged over 3000 years has been subtracted from the longitude. Results shown in the top, middle, and bottom panels were obtained with the programs FSHEP, FSHEPRES, and FSHEPSIM.

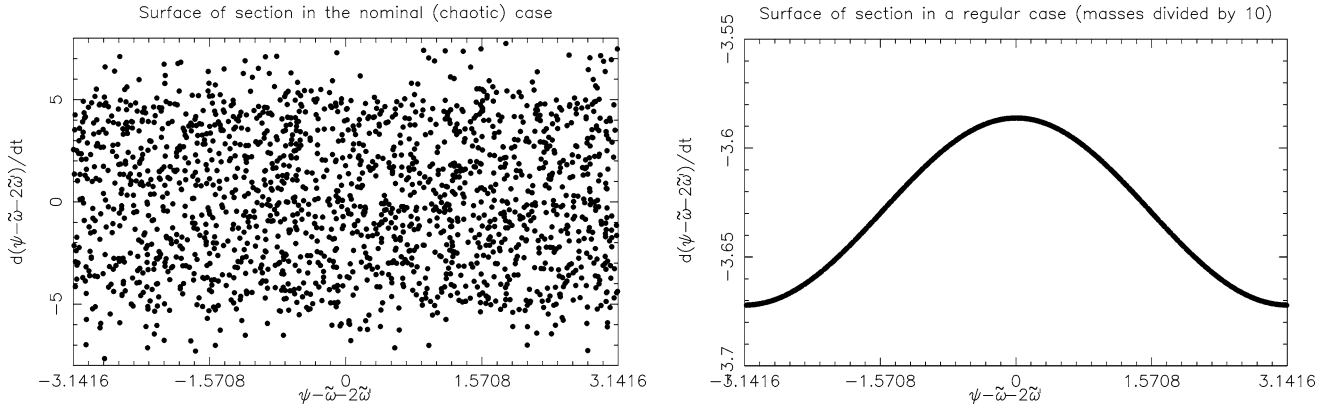

Fig. 8. Surfaces of section obtained by plotting $(\psi - \varpi - 2\varpi', \dot{\psi} - \dot{\varpi} - 2\dot{\varpi}')$ at each time of periapsis alignment over 3000 years. Units are radians and radians per year. Computations were made with FSHEPSIM, for the left panel with the nominal value of 0.63 g cm^{-3} for the satellite density. For the right panel, the density was reduced by a factor of 10 in order to obtain an integrable example to contrast with the chaotic one shown above.

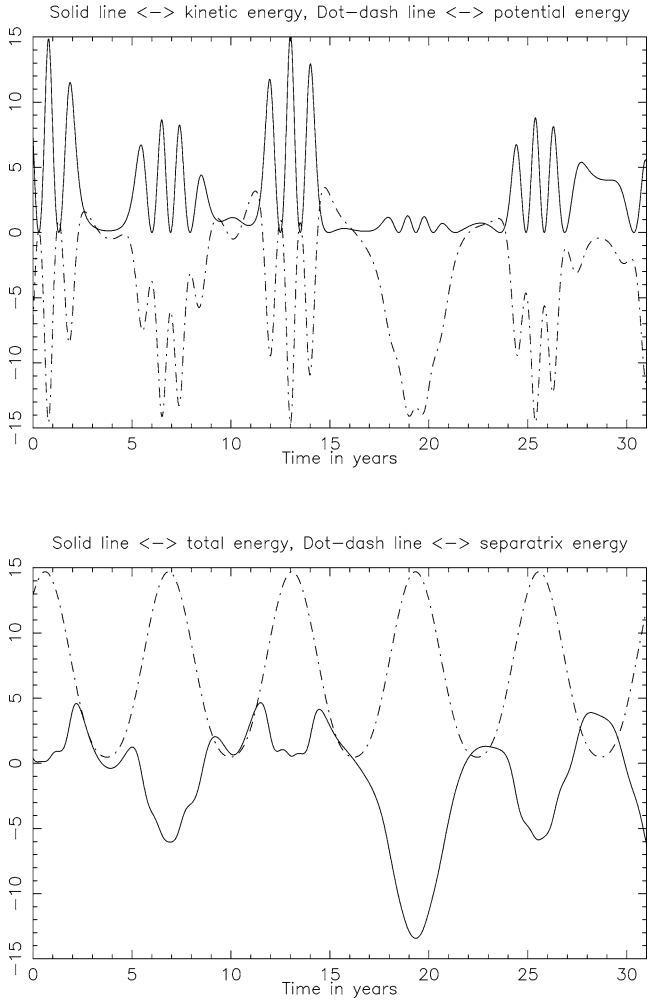

Fig. 9. The solid and dashed lines in the top panel show the kinetic and potential energies associated with the critical argument of the dominant ($q = 3$) member of the resonant quartet. The lower panel offers a comparison between the total energy, plotted as a solid line, and the energy on the separatrix, plotted as a dashed line. The unit of energy in these figures is (degrees year^{-1})^2.

and that $\Delta(t) \ll 1$. If $|A(t)|$ were much larger than $\dot{\varpi} - \dot{\varpi}'$, the evolution of Φ_3 would be governed by a pendulum equation with a slowly varying restoring force.[12] To pursue this picture, we compute the pendulum's kinetic and potential energies

$$KE = \frac{1}{2}\left(\frac{d\Phi_3}{dt}\right)^2, \tag{26}$$

$$PE \equiv -A^2(t)\cos\big[\Phi_3 + \Delta(t)\big]. \tag{27}$$

Computations of these quantities over five precessional cycles are displayed in the upper panel of Fig. 9. Corresponding plots of the total energy and the energy on the separatrix are shown in the lower panel. These confirm that two separatrix crossings occur during most precessional cycles.

[12] In reality, the maximum value of $A(t)$ is about $3.8(\dot{\varpi} - \dot{\varpi}')$.

Acknowledgments

This research was supported by NASA Planetary Geology and Geophysics grant 344-30-55-07 and by NSF grant AST-0098301. We are grateful to two anonymous referees and especially to Dr. K. Tsiganis for many illuminating comments that resulted in what we hope is an improved paper.

References

Borderies, N., Goldreich, P., Tremaine, S., 1984. Unsolved problems in planetary ring dynamics. In: Greenberg, R., Brahic, A. (Eds.), Planetary Rings. Univ. of Arizona Press, Tucson, AZ, pp. 713–734.

Borderies-Rappaport, N., Longaretti, P.-Y., 1994. Test particle motion around an oblate planet. Icarus 107, 129–141.

Campbell, J.K., Anderson, J.D., 1989. Gravity field of the saturnian system from *Pioneer* and *Voyager* tracking data. Astron. J. 97, 1485–1495.

French, R.G., McGhee, C.A., Dones, L., Lissauer, J.J., 2003. Saturn's wayward shepherds: the perigrinations of Prometheus and Pandora. Icarus 162, 144–171.

(GR03) Goldreich, P., Rappaport, N., 2003. Chaotic motions of Prometheus and Pandora. Icarus 162, 391–399.

Murray, C.D., Dermott, S.F., 2001. Solar System Dynamics. Cambridge Univ. Press, pp. 551–552.

Nicholson, P.D., Hamilton, D.P., Matthews, K., Yoder, C.F., 1992. New observations of Saturn's coorbital satellites. Icarus 100, 464–484.

Thomas, P.C., 1989. Shapes of small satellites. Icarus 77, 248–274.